In Situ Measurements of Microphysical Properties of Mid-latitude and Anvil Cirrus

R. Paul Lawson*, Brad A. Baker and Bryan L. Pilson

SPEC Incorporated, Boulder, C0 80301 USA

Abstract - Research aircraft measurements of detailed microphysical properties of mid-latitude cirrus, mid-latitude anvil and tropical anvil clouds are discussed. A cloud particle imager (CPI) and standard optical probes are used to generate composite particle size distributions, ice water content, effective radius, extinction coefficient and particle habit in 13 mid-latitude cirrus clouds. Over 250,000 ice particles are classified by crystal habit. The measurements show that the predominant crystal type by number in anvils is small spheroidal particles, occurring in concentrations from 0.1 to 5 cm^{-3}. In cirrus, the predominant crystal type, weighted by mass is the bullet rosette. Cirrus microphysical properties are compared with mid-latitude and tropical anvils, which are found to have one to two orders of magnitude higher concentrations of ice crystals. Bullet rosettes are rare in anvils. Chains of small ice particles, aggregates and complex crystals are common in mid-latitude anvils, but far less-common in tropical anvils. The difference may be a function of the higher electric fields in mid-latitude anvils, which may also lead to the formation of chains of small ice particles.

Keywords: Cirrus, wave clouds, anvils, ice crystals, cloud microphysics, cloud radiative properties

1. INTRODUCTION

The relatively recent development of the cloud particle imager (CPI) has led to improvement in measurements of the size and shape of cloud particles. This in turn has led to an improved ability to distinguish water drops from ice particles and to identify the habits of ice crystals (e.g., Korolev et al. 1999; Lawson et al., 2001; Heymsfield et al. 2002). Here we discuss aircraft data collected in cirrus and anvil clouds. The primary research platform used in these studies is the SPEC Learjet, however, limited additional data are presented that were collected by the NASA WB-57 and DC-8, and the University of North Dakota (UND) Citation.

Our analysis of particle types in cirrus and anvil clouds shows that the shapes of particles in mid-latitude cirrus are distinctly different than particle shapes in anvil clouds. Also, the data show that the shapes of particles in mid-latitude (continental) anvils are different than those in tropical (maritime) anvils. Differences in particle shapes has a significant impact on microphysical retrievals based on remote sensors (Stevens et al. 1990).

2. CIRRUS CLOUDS

Table 1 shows the date, time, cloud base altitude and temperature, cloud top altitude and temperature and the duration in cloud for 13 flights in cirrus clouds investigated by the SPEC Learjet over Utah, Colorado and Oklahoma. The cirrus clouds were all synoptically or orographically generated, not remnants of convection. Since the locations, Utah, Colorado and Oklahoma are downwind of major mountain ranges, some of the cirrus may have been orographically enhanced, but this is difficult to quantify. Except for one case, 11 November 1998, the flights were conducted in relatively thin, cold-based cirrus. The 11 November 1998 flight was near Salt Lake City, Utah and is an example of a deep cirrus cloud system that was likely orographically enhanced.

Figure 1 shows average PSDs based on number concentration and mass, and a histogram of particle habits based on measurements made in the 13 cirrus clouds listed in Table 1. The measurements are averaged over ± 5 ° C temperature ranges centered around –35, -45 and –55 ° C. The data in Figure 1 show that particle concentration, size, IWC and extinction coefficient all decrease with increasing altitude, and that the predominant particle type in cirrus is the bullet rosette. However, there are very high number concentrations of small (< 50 μm quasi-spheroidal particles and relatively high concentrations of slightly larger irregular shapes. While most of the data shown in Table 1 were collected in relatively thin (< 2 km) cirrus, the flight on 11/16/98 was conducted in cirrus that was about 4 km deep. As shown in Figure 2, the particle shapes near the top of the cloud are dominated by small quasi-spheroidal particles, irregulars, budding rosettes (i.e., rosettes with short arms) and some columns. Budding rosettes and rosettes comprise most of the particles in the middle two-thirds of the cloud, while near the bottom of the cloud there exist complex shapes that have sideplanes and/or are aggregates of crystals.

Figure 3 shows a plot of length versus area for rosette crystals in cirrus where the different colors correspond with rosettes with different temperatures. The plot shows that the relationship of length to area is very systematic and predictable in the cirrus clouds studied. This relationship can be used in models where PSDs are generally specified by measurements of particle size, and particle area is the most useful parameter in radiative transfer retrievals and simulations.

3. ANVIL CLOUDS

Here we present some examples of PSDs and particle types in thunderstorm anvils observed by the SPEC Learjet in mid-latitudes, the NASA WB-57 and UND Citation in Florida, the ARA Egrett in Darwin and the NASA DC-8 in Kwajalein. The particle shapes found in anvils are very different than those observed in mid-latitude cirrus. Particles observed in the anvils of mid-latitude, Florida and Darwin thunderstorms tend to contain a high percentage of aggregates and chain-like crystals. Figure 4 shows examples of CPI images observed in continental storms in Colorado, Florida, Darwin, and in a maritime tropical storm near Kwajalein. An intensive visual analysis of the images revealed that about 30% of the CPI images in the continental anvils are comprised of aggregates, or complex chains of particles that appear to be aggregates or heavily rimed particles, while less than 1% of the images in the Kwajalein anvil were aggregates. In addition, 2 to 6% of the images in the continental storms appeared to be doublets or chains of small particles (Table 2). These "chains" are very similar in appearance to chains of ice crystals observed in a cold chamber under a high electric field.

* Corresponding Author: Dr. R. Paul Lawson (plawson@specinc.com). This work has been funded by the U.S. National Science Foundation and National Aeronautics and Space Administration.

Table 1.
Cloud base and cloud top altitude, temperature and duration in cloud for cirrus clouds investigated by the SPEC Learjet.

Date	Cloud Base	Cloud Top	Temperature
11/16/98	FL 250	FL 390	-28 C to -50 C
3/1/00	FL 245	FL 300	-31 C to -39 C
10/16/00	FL 280	FL 410	-34 C to -61 C
10/19/00	FL 330	FL 350	-48 C to -50 C
12/1/00	FL 370	FL 390	-61 C to -63 C
5/1/01	FL 290	FL 350	-34 C to -48 C
5/25/01	FL 330	FL 370	-51 C to -59 C
10/30/01	FL 280	FL 350	-33 C to -49 C
10/31/01	FL 290	FL 310	-37 C to -40 C
11/7/01	FL 290	FL 350	-37 C to -50 C
11/12/01	FL 310	FL 370	-44 C to -58 C
11/14/01	FL 330	FL 350	-50 C to -54 C
11/21/01	FL 320	FL 350	-46 C to -55 C

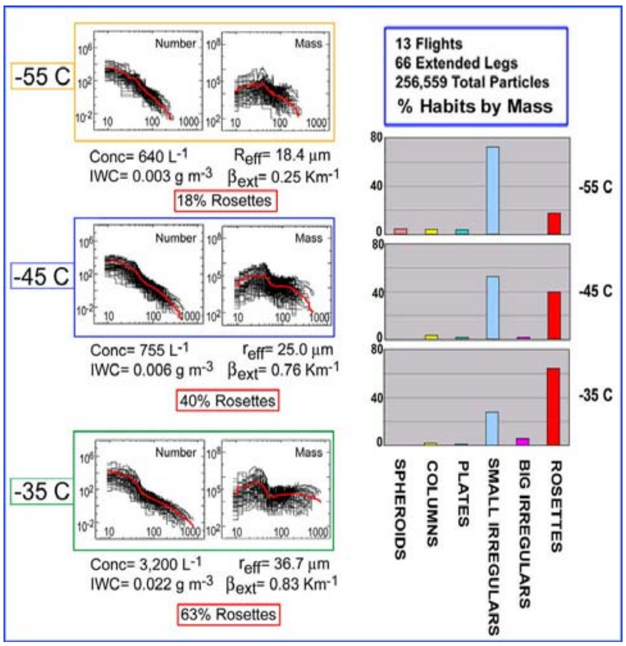

Figure 1. On the left are PSDs weighted by number concentration and mass concentration for three different temperature levels in the 13 cirrus clouds shown in Table 1. Each PSD shown in black is a leg average and the red PSD is the mean of all of the legs. At right are histograms where particle types are weighted by particle mass and only particles > 50 µm have been classified.

Table 2.
Ice particle characteristics in Continental and Maritime Anvils.

Airmass	Location	# Particles Counted	% Chains	% Doublets	% Other Aggregates	Temperature
Continental	Colorado 6-8-01a	3400	3	6	25	-47 C
Continental	Colorado 6-8-01b	1400	2	5	32	-47 C
Continental	Colorado 6-8-01c	3800	2	4	28	-47 C
Maritime	Kwajalein 8-3-98	3900	0	1	0.4	-40 to -60 C
Maritime	Kwajalein 8-25-98	1700	0	0.1	0.5	-55 C
Maritime	Kwajalein 9-2-98	11000	0	2.3	1.4	-5 to -40 C

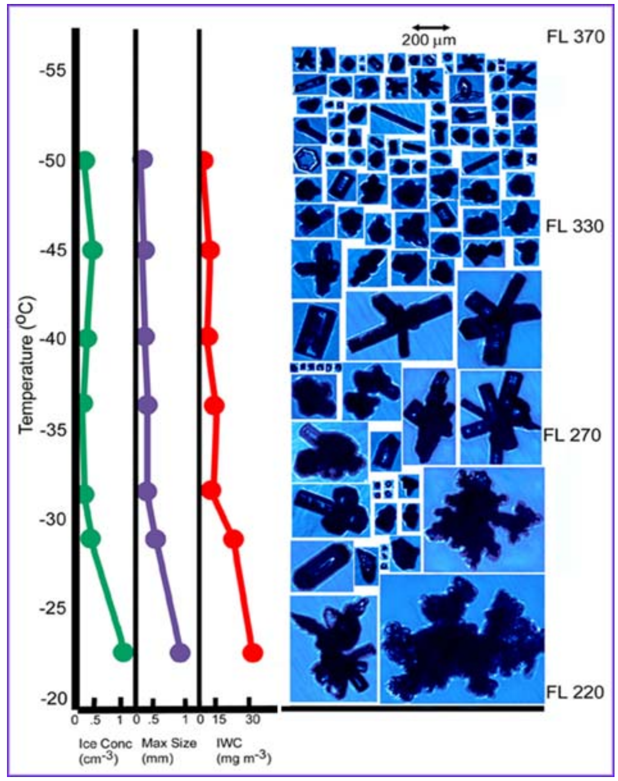

Figure 2. Vertical profile showing examples of CPI images and microphysical data in a deep cirrus cloud (11/16/98). The values of ice particle concentration (Ice Conc), maximum particle size (Max Size) and ice water content (IWC) are 10-s (15 km) average values.

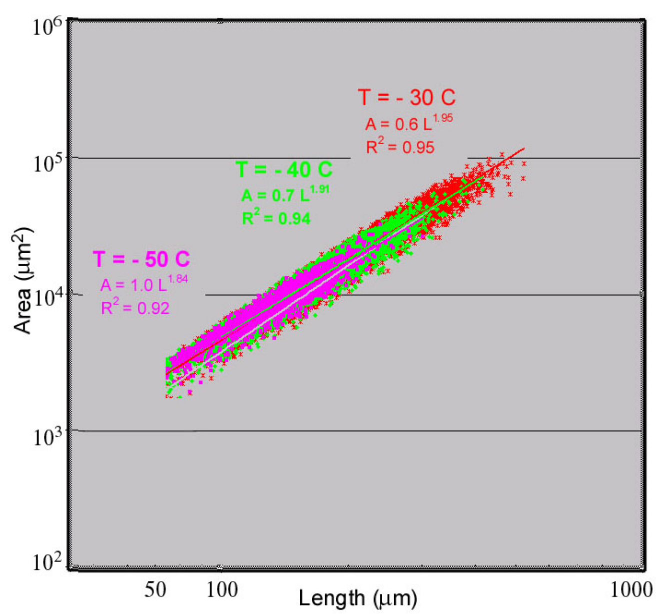

Figure 3. Plot of CPI particle length versus particle area. The data points are color-coded as a function of temperature for the 13 cirrus clouds shown in Table 1. Best fit equations and correlation coefficients are shown for each temperature.

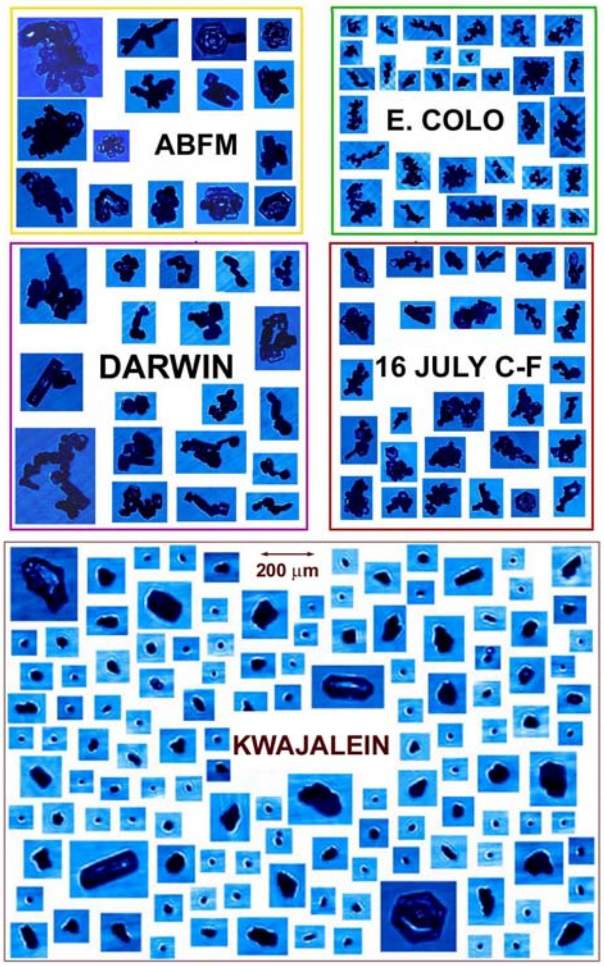

Figure 4. Examples of CPI images from (top four panels) continental anvils and (bottom panel) maritime anvil.

Figure 5, which is reproduced from Saunders and Wahab (1975), shows examples of chains of ice particles in the presence of a 100 KV m^{-1} electric field, which is typical of anvils with high electrical activity (i.e. lightning). All of the locations where chains of ice particles were observed typically have high occurrence of lightning, while storms near Kwajalein are typically devoid of lightning (Christian et al. 2003). The aggregates of small ice particles observed in continental anvils strongly resemble the chains formed in the laboratory under high electric fields. This strong resemblance and the observation that no chains are observed in the relatively weak electric fields of tropical anvils leads one to believe that electric charge is involved in the aggregation process. However, more quantitative measurements of electric field in anvils and correlations with in situ measurements are needed.

Regardless of whether the anvils are continental or maritime, the particle shapes in anvils bear virtually little resemblance to the shapes of particles in mid-latitude cirrus clouds. This can be explained through the realization that most of the ice crystals in thunderstorms are nucleated in the updrafts at temperatures > -30 ° C. The ice particles are then carried up into the anvil. On the other hand, cirrus clouds are formed in situ at temperatures that are generally < - 30 ° C, so polycrystalline structures such as rosettes are expected. The shapes of the particles in cirrus clouds, compared with those in anvils, will result in significantly substantially different phase functions (Lawson et al. 1998). The different phase functions will have a significant impact on calculations of radiative transfer.

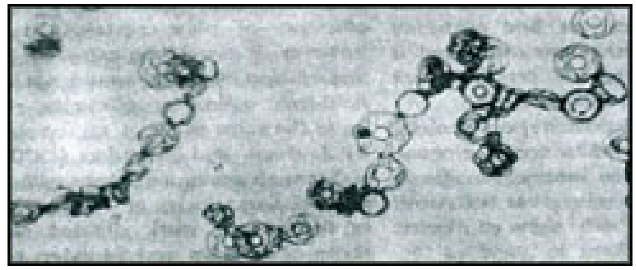

Figure 5. Examples of "chains" of ice particles formed in a cloud chamber under the influence of high (100 KV m^{-1}) electric field (after Saunders and Wahab 1975).

In addition to the striking difference in particle shapes, there are significant differences in particle concentration and the optical properties of anvils compared with cirrus clouds. Figure 6 shows a pictorial depiction of a Learjet flight through three regions of a small anvil cloud in Eastern Colorado. **A** and **B** show areas where the Lear encountered regions with, respectively, high concentration of large ice with low concentration of small ice, and low concentration of large ice with very high concentration of small ice, approaching 100 cm^{-3}. In the small particle region (**B**), the integrated IWC from the FSSP is in general agreement with the Nevzorov IWC measurement, and in the large particle region (**A**), the Nevzorov IWC agrees better with the 2D-C integrated IWC. This agreement provides further support for the validity of the particle measurements. Region **B** confirms the existence of very high concentrations of small ice particles, with concentrations approaching those reported by Strapp et al. (1999), who measured concentrations exceeding 200 cm^{-3} and IWC values in excess of 2 g m^{-3} in an anvil near the center of strong convection. These region with high ice concentrations, which are located in or in very close proximity to the convection, are likely the result of homogeneous freezing of cloud drops in the updrafts. Strapp et al. (1999) found excellent agreement between the IWC computed from the integrated PSD and the Nevzorov IWC. The measurements shown here and those reported by Strapp et al. (1999) suggest that very high concentrations of small ice particles do exist in Anvils, and that they cannot always be explained by large particles shattering on the inlets of the probes, (although particle shattering may be contributory or even dominant under some circumstances).

Figure 7 shows particle size distributions, examples of CPI images and derived parameters from two levels in an anvil investigated during the NASA CRYSTAL-FACE field campaign in southern Florida. The particle concentrations are lower than in the continental anvil in Figure 6. The Florida penetrations were at higher elevations and farther from the center of convection than the anvil shown in Figure 6. The lower ice concentrations are expected, because as shown by Lawson et al. (1998), particle concentration generally decreases rapidly in anvils with distance from the center of convection and with increasing altitude.

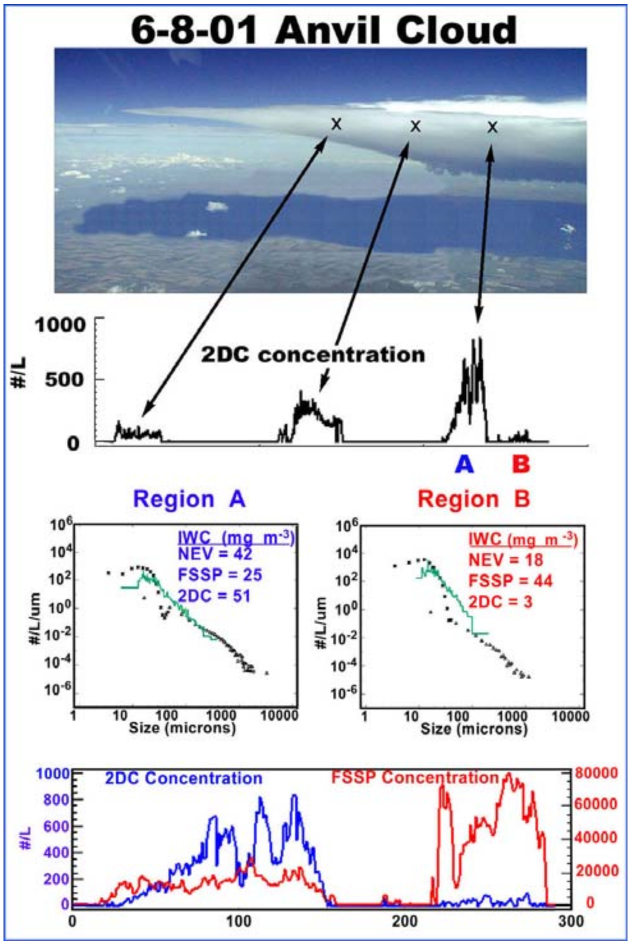

Figure 6. The x's in the photos show where the SPEC Learjet penetrated a small anvil cloud in Eastern Colorado. Regions **A** (blue) and **B** (red) show areas where the Lear encountered, respectively, high concentration of large ice with low concentration of small ice, and low concentration of large ice with very high concentration of small ice, approaching 100 cm^{-3}. The Nevzorov IWC is compared with the integrated IWC from the 2D-C in region **A**, and with the FSSP integrated IWC in region **B**.

Figure 8 shows particle size distributions, examples of CPI images and derived parameters from two levels in an anvil investigated during the NASA KWAJEX field campaign near Kwajalein. Here, the DC-8 penetrated a relatively old, weak portion of the thunderstorm outflow. The particle concentrations, IWC and optical properties are similar to those found in the C-F anvil, but as previously discussed, the shapes of the particles are much different. Instead of aggregates, complex crystals and chains of small particles found in continental anvils, the large majority of the particles in tropical anvils are single crystals that have irregular, blocky shapes, with only occasional hex-shaped crystals.

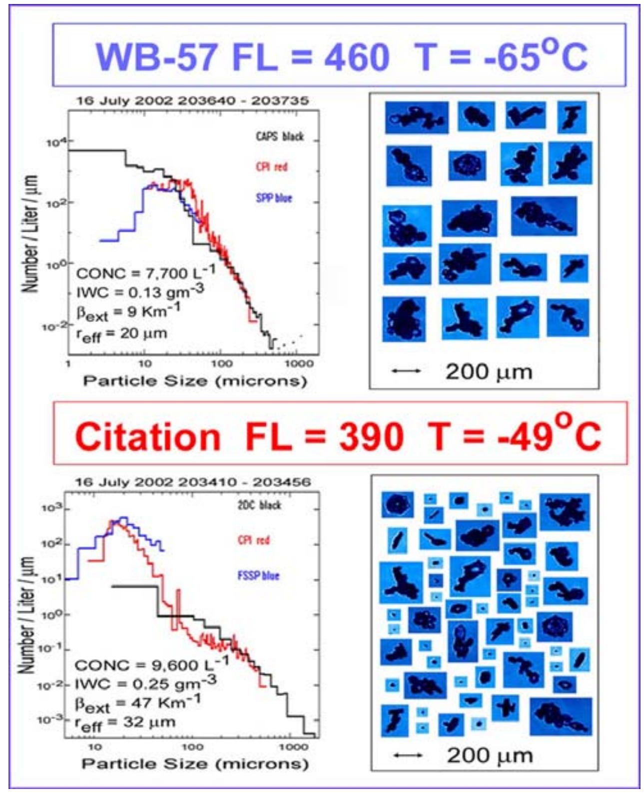

Figure 7. PSDs, CPI images, values of total particle concentration (conc), ice water content (IWC), extinction coefficient (β_{ext}) and effective radius (r_{eff}) derived from the composite PSDs for two levels in an anvil studied in Florida during the CRYSTAL-FACE experiment.

5. SUMMARY

Table 3 lists summary microphysical properties of mid-latitude cirrus, continental and tropical anvils based on measurements discussed in this paper.

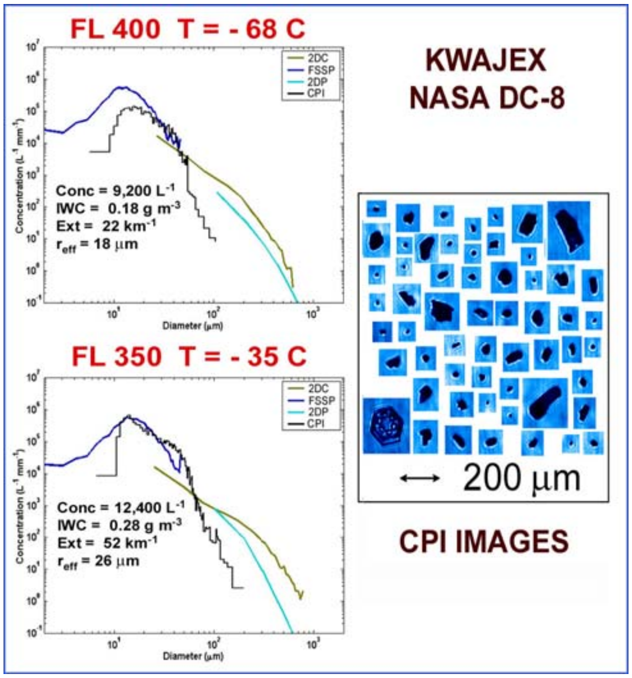

Figure 8. PSDs, CPI images, values of total particle concentration (conc), ice water content (IWC), extinction coefficient (β_{ext}) and effective radius (r_{eff}) derived from the composite PSDs for two levels in an anvil studied near Kwajalein during the NASA TRMM KWAJEX experiment.

Table 3.

Typical values of total particle concentration (Conc.), ice water content (IWC), effective radius (r_{rff}), extinction coefficient (β_{ext}) and particle type for mid-latitude cirrus clouds, Continental and Maritime anvil clouds.

Cloud Type	*Conc. cm^{-3}*	*IWC $g\ m^{-3)}$*	*r_{eff} μm*	*β_{ext} km^{-1}*	*Predominant Particle Type*
Mid-latitude Cirrus	0.1 to 10	0.001 to 0.05	10 to 30	0.1 to 1	Rosettes and Budding Rosettes for –55 < T > -25 C, Small Spheroids, few columns, virtual no plates
Cont. Anvil	10 to 100	0.1 to 2.0	10 to 50	10 to 100	Irregulars, Aggregates, Rimed particles, sideplanes, Small Spheroids, Chains of small particles
Maritime Anvil	10 to 100	0.1 to 1.0	10 to 30	10 to 100	Blocky, single-particle Irregulars, small spheroids, few columns and plates

REFERENCES

Christian, H. J., et al., 2003: Global Frequency and Distribution of Lightning as Observed from Space by the Optical Transient Detector, *J. Geophys. Res.*, **108** (D1**),** 4005.

Gayet, J.-F., F. Auriol, S. Oshchepkov, F. Scröeder, C. Duroure, G. Febvre, J.-F. Fournol, O. Crépel, P. Personne and D. Daugereon, 1998: In situ measurements of the scattering phase function of stratocumulus, contrails, and cirrus. *Geophys. Res. Letters*, **25**, 7, 971-974.

Heymsfield, A.J., S. Lewis, A. Bansemer, J. Iaquinta, L.M. Miloshevich, M. Kajikawa, C. Twohy and M.R. Poellot, 2002: A General Approach for Deriving the Properties of Cirrus and Stratiform Ice Cloud Particles. *J. Atmos. Sci.*, **59**, 3-29.

Korolev, A.V., G.A. Isaac and J. Hallett, 1999: Ice particle habits in Arctic clouds. *Geophys. Res. Letters*, **26**, *9*, 1299-1302.

Lawson, R. P., A. J. Heymsfield, S. M. Aulenbach and T. L. Jensen, 1998: Shapes, sizes and light scattering properties of ice crystals in cirrus and a persistent contrail during SUCCESS. *Geo. Res. Let.*, **25**(9), 1331-1334.

Lawson, R.P., B.A. Baker, C.G. Schmitt and T.L. Jensen, 2001: An overview of microphysical properties of Arctic clouds observed in May and July during FIRE.ACE. *J. Geophys. Res.*, **106**, 14,989-15,014.

Mishchenko, M. I., W. B. Rossow, A. Macke and A. A. Lacis, 1996: Sensitivity of cirrus cloud albedo, bidirectional reflectance, and optical thickness retrieval accuracy to ice-particle shape. *J. Geophys. Res.*, **101**, D12, 16973-16985.

Sassen, K., J.M. Comstock, Z. Wang and G. Mace, 2001: Cloud and aerosol research capabilities at FARS: the Facility for Atmospheric Remote Sensing. *Bull. Of Amer. Meteorol. Soc.*, **82**, 1119-1138.

Saunders and Wahab, 1975: The Influence of Electric Fields on the Aggregation of Ice Crystals, *J. Meteor Soc Japan*, 53, 121-126.

Stephens, G. L., Tsay, S-C, Stackhouse, P. W. and Flatau, P. J., 1990: The relevance of the microphysical and radiative properties of cirrus clouds to climate and climatic feedback. *J. Atmos. Sci.*, **47**, 1742-1753.

Strapp, J.W., P. Chow, M. Maltby, A.D. Bezer, A. Korolev, I. Stromberg and J. Hallett, 1999: Cloud microphysical measurements in thunderstorm outflow regions during Allied/BAE 1997 flight trials. AIAA 00-0498.

Takano, Y. and K. N. Liou, 1995: Radiative transfer in cirrus clouds; Part III: Light scattering by irregular ice crystals. *J. Atmos. Sci.*, **52**, 818-837.